Soft Matter

Accepted Manuscript

ROYAL SOCIETY OF CHEMISTRY

www.rsc.org/softmatter

ARTICLE TYPE www. rsc.org/xxxxxx | XXXXXXXX

'Soft' amplifier circuits based on field-effect ionic transistors

Niels Boon,[a], and Monica Olvera de la Cruz[b]

Received Xth XXXXXXXXXX 20XX, Accepted Xth XXXXXXXXX 20XX
First published on the web Xth XXXXXXXXXX 200X
DOI: 10.1039/b000000x

Soft materials can be used as the building blocks for electronic devices with extraordinary properties. We introduce a theoretical model for a field-effect transistor in which *ions* are the gated species instead of electrons. Our model incorporates readily-available soft materials, such as conductive porous membranes and polymer-electrolytes to represent a device that regulates ion currents and can be integrated as a component in larger circuits. By means of Nernst-Planck numerical simulations as well as an analytical description of the steady-state current we find that the responses of the system to various input voltages can be categorized into ohmic, sub-threshold, and active modes. This is fully analogous to what is known for the electronic field-effect transistor(FET). Pivotal FET properties such as the threshold voltage and the transconductance crucially depend on the half-cell redox potentials of the source and drain electrodes as well as on the polyelectrolyte charge density and the gate material work function. We confirm the analogy with the electronic FETs through numerical simulations of elementary amplifier circuits in which we successfully substitute the electronic transistor by an ionic transistor.

More than half a century of progress in the field of silicon-based semiconductor electronics has resulted in incredibly small devices that process data at dazzling speeds. Recent years have nonetheless seen a vast amount of research and progress in the field of electronics that are made out of organic materials. This development is not driven by an interest in a further increase of computational power but rather focusses on creating devices with properties mostly unseen in conventional electronics such as flexibility, transparency, solvent processability, or biodegradability[1–8]. As an alternative to devices that use electron currents, it was demonstrated recently that transparent electrostatic loudspeakers can be constructed by converting electric sound signals into ion currents which can then run through hydrogels[9]. More fundamentally, others have achieved rectification of ion currents through the interface between polyelectrolyte gels that have oppositely charged polymer backbones: it was found that a voltage difference applied to a pair of electrodes is able to induce a continuous current in one direction, yet the interface almost completely blocks the current in the other direction. That property therefore enables the construction of ionic diodes[10–13] made from soft materials. Not only rectification but also the *gating* of ion currents happens abundantly in ion channels in biological membranes[14], and gating has also been achieved in nanodevices[15]. Despite this emerging analogy with semiconductor electronics, an ionic analogue of a *transistor* that can be integrated into larger circuits has not yet been investigated; transistors form the heart of almost any modern-electronics device. Typically, field-effect transistors (FETs) provide the signal processing capability that many of these devices need.

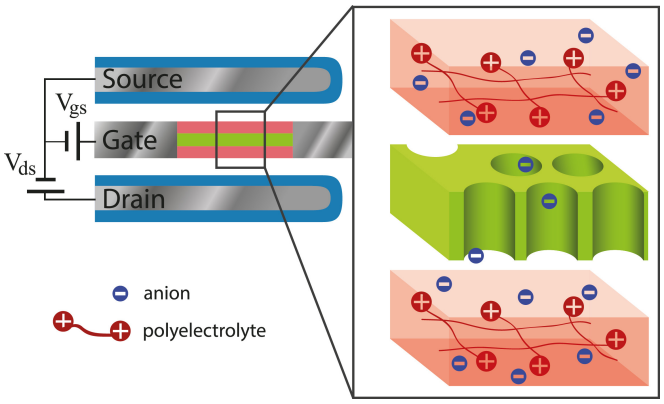

Fig. 1 The model system that we consider, showing the porous gate material in green which is sandwiched by layers of cationic polyelectrolyte, corresponding to the red regions. The electronic current converts to an ion current (and back) at the AgCl/Ag redox surfaces at the source and the drain, which are illustrated in blue. The device is operated by applying external voltage differences V_{gs} and V_{ds} to the electrodes.

In this work we consider a theoretical model for a field-effect *ionic* transistor and we show by means of Nernst-Planck numerical simulations that devices like this will enable the construction of amplifier circuits due to a striking analogy

[a] *Department of Materials Science and Engineering, Northwestern University, Evanston, Illinois 60208, USA; E-mail: n.boon@northwestern.edu*
[b] *Department of Materials Science and Engineering, Northwestern University, Evanston, Illinois 60208, USA; E-mail: m.olvera@northwestern.edu*

with the electronic FET[16], which is used as inspiration for our model. The working of the latter device relies on a semiconducting strip that is placed in the close proximity of a so-called gate electrode. The electrostatic potential of that electrode is able to regulate the density of delocalized electrons in the underlying semiconductor and as a result the electronic conductance of the strip can be made to vary over orders of magnitude by changing the gate potential. We, however, will not be interested in electrons but aim at a device in which *ions* are gated. Instead of electronic (semi-) conductors we will therefore consider soft-matter systems in which ions are the charge-carrying species in a solvent, such as water. Currents can be induced by creating chemical potential differences, for example by applying an external potential. The tendency of the ions to move down in chemical potential can be employed by requiring them to pass through a 'gate' to accomplish this. An adjustable barrier potential in the gate will determine the concentration of ions and as a result the rate at which ions are able to pass. This therefore controls the total current through the system. Since ions are charged it is possible to apply such a barrier potential by means of an electrode that is connected to an external voltage source. Nevertheless, because ions screen electric fields, only the ion concentration in the immediate proximity of the electrode can be affected in this way. Interesting candidates for the purpose of creating gates are therefore electronically conductive materials with an interconnected porous microstructure, such that an external potential can be set throughout the *entire* internal volume of the material and ions in the pores will respond to that by adjusting their number density. Materials with these properties are already of great interest for application in supercapacitors[17,18], and render them also applicable for the generation of power from salinity differences[19,20] or, oppositely, desalination[21]. The gating of ion currents has to the best of our knowledge never been investigated in the context of these materials. It is not clear how such materials can be used to construct transistors and in which way the resulting devices could be applied as signal amplifiers. This is because the working of the electronic FET crucially depends on the quantized energy levels of the semiconductor, whilst classical physics suffices in the description of ion motion. Nanoporous structures that can be applied in supercapacitors predominantly have carbon as the main component. Such materials combine electronic conductance with a high degree of chemical stability. To gate ion currents we also require the possibility of these materials to be shaped into thin porous membranes such that the ions can move through at high rates. Recent work suggests that such membranes might also be realized using graphene-oxide[22] or block co-polymers[23]. Presumably many other candidates either already exist or can be tailored[24], yet we emphasize here that creating materials with pore sizes that are comparable to the Debye screening length is a challenging fabrication requirement in general. In this work we assume the gate takes the form of a thin nanoporous membrane that is electronically conductive.

In electronic FETs the charge carriers are the electrons, yet for a typical ionic solution both the cations and the anions tend to move in opposite directions under the influence of electric fields. In experiments in which rectification of ion currents was observed, this symmetry had been broken by replacing ordinary salt by polyelectrolyte gels[10–12]. The fixed charged backbone of the polymer does not contribute to the current, leaving the counterions the only current-carrying species[25]. Analogously, we include layers of polyelectrolyte gels on both sides of the gate material, as is shown in Figure 1. Its fixed cationic charge density n_+ ensures that the only mobile charge carriers are the anionic counterions which are required for the global charge neutrality. We do not include additional salt in our model. Fully analogous to the electronic FET, one may place electrodes in osmotic contact with either side of the polyelectrolyte-gate-polyelectrolyte sandwich to induce electric fields and thus a tendency for charge carriers to move through the system. Nevertheless, a voltage difference over those electrodes does not induce a very sustainable current since the ions will redistribute to accommodate towards any new external field, after which the current readily vanishes. Currents can however be kept going through redox reactions at the electrodes; in this way one electrode can act as an ion source where the ions are high in chemical potential and the other can act as a drain where they are low in chemical potential. In this work we will focus on silver-chloride electrodes as they find wide utilization in electrochemistry as reference electrodes and have successfully been applied to create ionic diodes[11–13]. Chloride ions will be released at the source electrode due the addition of electrons, $\mathrm{AgCl}^{(\mathrm{s})} + e_- \leftrightarrow \mathrm{Ag}^{(\mathrm{s})} + \mathrm{Cl}_-^{(\mathrm{aq})}$, while at the drain electrode the reverse reaction in which electrons are released into the electrode dominates. The long-term depletion of Cl_- in the Ag/AgCl source electrode can be circumvented by a periodic redefinition of the source and the drain electrode, which will reverse the ion current. The equilibrium constants corresponding to redox reactions are expressed via half-cell potentials. The *absolute* redox half-cell potential E_{abs} equals the Fermi level of the electrons in the electrode when the solution is at zero electrostatic potential[26]. More generally, the redox chemical equilibrium between an electrode and the solution in its proximity yields that the electrode can be regarded as a constant-potential surface where

$$e(\psi - \Phi) = W - eE_{\mathrm{abs}} \tag{1}$$

relates the non-vanishing (Donnan) electrostatic potential ψ in the solution to the electrode potential Φ. Here, e is the elementary charge and W is the work function that quantifies the affinity of electrons to the electrode material[27]. For silver we

find $W = 4.30$ eV[28]. The Nernst equation relates E_{abs} of the AgCl electrode to the *absolute standard half-cell potential* via $E_{\text{abs}} = E^{\ominus}_{\text{abs}} - kT/e \log a_{\text{Cl}^-}$, where $a_{\text{Cl}^-} = \gamma c_- / c^{\ominus}$ is the activity of the chloride ions which can be expressed in terms of the concentration of the involved ion species c_- and the standard-state concentration $c^{\ominus} = 1$ mol/l. We will approximate the ions to behave ideally and therefore set the activity coefficient $\gamma = 1$ in this work. Values for $E^{\ominus}_{\text{abs}}$ relate to the standard hydrogen half-cell potentials $E^{\ominus}_{\text{she}}$ via $E^{\ominus}_{\text{abs}} \approx E^{\ominus}_{\text{she}} + 4.44V$[29] and the latter are well documented: we find $E^{\ominus}_{\text{abs}} = 4.66V$ for AgCl[30]. For a typical concentration, say c_- = 5 mM, the potential difference $(\psi - \Phi)$ between the solution and the electrode is negative and approximately -0.50 V. The system bridges this by forming a double layer of ionic charge in between, spanning a distance of a few nanometres.

An electrostatic potential difference between the source and the drain electrode can readily be set by an external voltage source V_{ds} such that $V_{\text{ds}} = \Phi_{\text{d}} - \Phi_{\text{s}}$, as Figure 1 illustrates. Analogously, the gate potential Φ_{g} can be set by a different voltage source between the source and the gate electrode, $\Phi_{\text{g}} - \Phi_{\text{s}} = V_{\text{gs}} - \Delta W/e$. Here $\Delta W/e$ is the Volta potential between the gate and the source which is a materials property resulting from the work function difference $W_{\text{g}} - W_s$ between the gate and source electrode material. The anion current through the polyelectrolyte-gate-polyelectrolyte sandwich can be estimated with the Nernst-Planck equation[27], which relates the time-dependent anion density c_- profiles to the gradients in the electrostatic potential. More accurate and predominantly more structure-specific theories for charge transport in polyelectrolytes and porous media exist[31–33], yet in this work we keep the equations as general as possible to elucidate the characteristic properties of ion gating in such devices. Steady-state solutions, yielding a constant ion current density j_{ds} in a system are generally found by $\frac{\partial c_-}{\partial t} = -\frac{\partial j}{\partial x} = 0$, with j the local current density, x the spatial coordinate perpendicular to the layers and t the time. In the polyelectrolyte region the ion current density is determined by $j = -D_{\text{p}} \left(\frac{\partial c_-}{\partial x} - \frac{e}{kT} c_- \frac{\partial \psi}{\partial x} \right)$, where D_{p} the diffusion constant in the polyelectrolyte. We will assert that the characteristic pore size in the gate region is smaller than the Debye screening length such that the electrostatic potential can be approximated to be constant there, and as a result the current will be driven by a concentration gradient only: $j = -\eta D_{\text{g}} \frac{\partial c_-}{\partial x}$ and $\eta \frac{\partial c_-}{\partial t} = -\frac{\partial j}{\partial x}$, with D_{g} the effective diffusion constant in the gate[34]. The porosity η is the effective volume fraction that is available to the ions. The boundary conditions on the polyelectrolyte-gate-polyelectrolyte system are set by $c_-(0) = c_-(L) = n_+$, i.e. we will not consider the diffuse layers at the redox electrodes, as they could have a complicated microstructure. It is sufficient to assume that the electrodes are at direct contact with the system and we therefore assert local chemical equilibrium at both ends of the sandwich with each of the electrodes; we use Eq. (1) and choose Ψ relative to the source electrode, $\Phi_s \equiv 0$ such that $\Psi(0) = W_s/e - E^{\ominus}_{\text{abs}} + (kT/e)\log(n_+/c^{\ominus})$ and $\Psi(L) = \Psi(0) + V_{\text{ds}}$. In the gate region one finds $\Psi(x) = V_{\text{gs}} - \Delta W/e$. The gradient of the electrostatic potential must satisfy the Poisson equation $\frac{e}{kT}\frac{\partial^2 \psi}{(\partial x)^2} = -4\pi\lambda_{\text{B}}(n_+ - c_-)$, where $\lambda_{\text{B}} \approx 0.7$ nm is the Bjerrum length in water, and n_+ is the positive charge density in the polyelectrolyte backbone which vanishes in the gate. All the counterions are assumed to be chloride. Note that the electronic current to the source and the drain electrodes equals $-j(0)eA$ and $j(L)eA$ respectively, where A is the cross-section area of the device. The derivative of the net amount of electronic charge in the gate region gives the electronic current to the gate, which will vanish in a steady state. That distribution of electronic charge in the gate can be calculated from the constant-potential restriction, yielding that inside the gate this charge density should balance the ionic charge density such that the electric field vanishes.

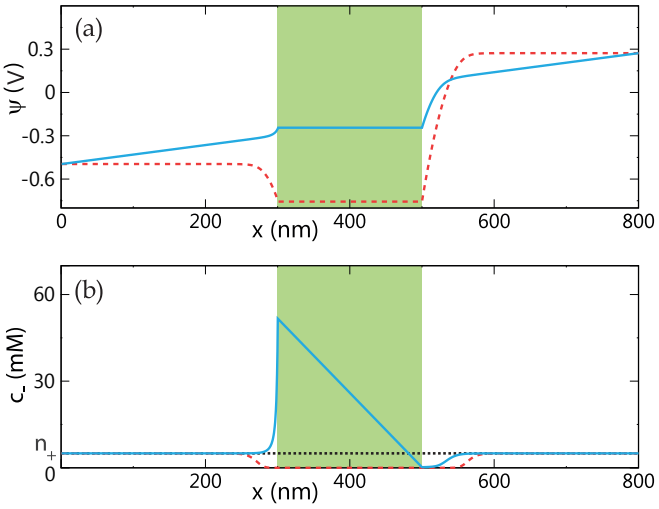

Fig. 2 The electrostatic potential (a) and the anion-density (b) profiles throughout the polyelectrolyte-gate-polyelectrolyte sandwich for $V_{\text{ds}} = 0.77$ V, yielding a current of anions in the positive direction. The full lines show results for $V_{\text{gs}} = +0.26$ V and the dashed lines correspond to $V_{\text{gs}} = -0.26$ V. The corresponding steady-state current densities are $j_{\text{ds}}e = 12.4$ mA/mm^2 and $j_{\text{ds}}e = 4 \cdot 10^{-5}$ mA/mm^2 respectively.

Figure 2 shows the resulting steady-state electrostatic potential and the anion profiles for $V_{\text{ds}} = 0.77$ V, while considering two values for the gate potential; $V_{\text{gs}} = -0.26$ V and $V_{\text{gs}} = +0.26$ V. Results were obtained for a system with a gate region of thickness $L_{\text{g}} = 200$ nm having a porosity $\eta = 0.5$. There are two $L_{\text{p}} = 300$ nm polyelectrolyte layers with n_+ = 5 mM on either side. The gate material is assumed to be carbon and therefore we choose $W_{\text{g}} = 4.8$ eV, although the exact value for W_{g} will depend on the microscopic structure of the carbon

and its contaminations[35]. We use $D_g = D_p = 10^{-9}$ m^2/s in our numerical calculations. Figure 2a shows the resulting potential relative to the source electrode potential, displaying the vanishing electric field in the gate region, the double layers at the gate-polyelectrolyte interface, as well as the large regions in the polyelectrolyte where an electric field is a constant driving force for the ions. Figure 2b furthermore shows that in these regions the concentration gradient is close to zero as a consequence of the system reaching local charge neutrality, i.e. $c_- \to n_+$, outside the double-layer regions. In the gate the ion concentration decreases linearly, which is the result of a concentration gradient that is driving the current here. The resulting steady-state current density j_{ds} through the system, which is directly proportional to the slope of the concentration in the gate region, demonstrates a variation of over six orders of magnitude between our two choices for V_{gs} as is illustrated by the full and the dashed lines in Fig. 2. Whereas j_{ds} is thus highly dependent on variations in V_{gs}, we surprisingly find that it is almost completely *independent* on variations in V_{ds} for the parameters used in Fig. 2. This saturation of j_{ds} with respect to V_{ds} is a highly nonlinear effect that is not seen in ohmic devices in which current and voltage are directly proportional to each other. Interestingly, the latter is also observed in electronic FETs and is known as 'channel pinch off'. This is a pivotal property of FETs as it is advantageous to have j_{ds} completely decoupled from V_{ds} for amplification purposes.

To get a more fundamental understanding of the observed highly nonlinear response of the steady-state current to the electrode potentials V_{ds} and V_{gs} we will investigate the variation of the anion chemical potential μ_- throughout the system. We write the latter as $\mu_- = \mu_-^{\ominus} + kT\log(c_-/c^{\ominus}) - e\psi$, where $\mu_-^{\ominus}$ is a contribution independent of the concentration and the electrostatic potential. If the polyelectrolyte regions are large compared to the double layers at the gate/polyelectrolyte interface then most of the polyelectrolyte will be locally charge neutral and consequently the decrease of the anion chemical potential in each of the polyelectrolyte regions can be estimated by Ohms law: $\Delta\mu_p = -j_{ds}\, kTL_p/(n_+D_p)$. The anion concentration at the source side in the gate region can be related to the local chemical potential and its change throughout the gate is given by $\eta\Delta c_- = -j_{ds}L_g/D_g$. The latter relates to a decrease in the chemical potential $\Delta\mu_g$, yet note that $\Delta\mu_g$ will only depend on the relative change in c_-. Combined with the restriction that the total variation in the chemical potential from the source to the drain is $\Delta\mu = -eV_{ds}$, this results in a non-linear equation for the ion current, $\Delta\mu = 2\Delta\mu_p + \Delta\mu_g$. That equation can in principle only be solved numerically, yet it can be approximated by analytical equations throughout the entire parameter regime spanned by V_{ds} and V_{gs}.

We proceed by relating the steady-state electric current density $-j_{ds}e$ to the gate voltage V_{gs} in the saturated mode corresponding to Fig. 2, as is shown in Figure 3 where $j_{ds}e$ is plotted

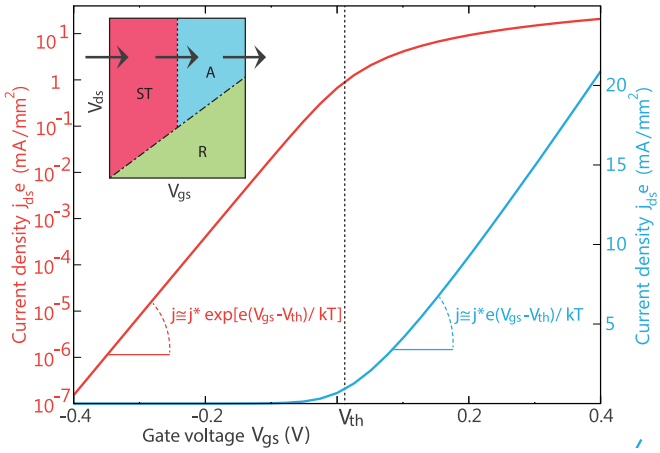

Fig. 3 The steady-state drain-source electric current density $j_{ds}e$ as a function of the gate-source voltage V_{gs}, shown on a logarithmic scale (red, left axis) and on a linear scale (blue, right axis). The inset illustrates the subdivision of the parameter space spanned by V_{gs} and V_{ds} into three modes, showing the sub-threshold(ST), active(A), and ohmic(R) mode. The arrows indicate the choice of parameters in the main graph. The dashed line at $V_{gs} = V_{th}$ indicates the transition from the sub-threshold to the active mode.

on both a linear and on a logarithmic scale. This reveals two different modes of operation: we find a *subthreshold mode* at low V_{gs} where the current density increases exponentially with V_{gs}, $j_{ds} \approx j_{ds}^* \exp[(V_{gs} - V_{th})e/kT]$, with a transition around $V_{gs} = V_{th}$ to the *active mode* where the current increases approximately linearly with V_{gs}, $j_{ds} \approx j_{ds}^*(V_{gs} - V_{th})e/kT$. This behaviour, which is confirmed by both our analytical approach and our numerical simulations, is very similar to what is known for the electronic FET[36]. However, for the field-effect ionic transistor, which we will refer to from now on as FEiT, the *threshold voltage* V_{th} and the *threshold current density* j_{ds}^* are found to be given by

$$V_{th} = \frac{W_g}{e} - E_{abs}^{\ominus} + \frac{kT}{e}\log\left(\frac{n_+}{c^{\ominus}}\frac{L_gD_p}{\eta L_pD_g}\right); \qquad (2)$$

$$j_{ds}^* = \frac{n_+D_p}{L_p}, \qquad (3)$$

respectively. For our choice of parameters we find $V_{th} = 11.7$ mV and $j_{ds}^*e = 1.6$ mA/mm^2 and therefore, in retrospect, the dashed and the full lines in Figure 2 thus correspond to choices for V_{gs} in the subthreshold and the active mode respectively. Our analytical approach confirms that j_{ds} is decoupled from V_{ds} in these modes, yet we find that the FEiT can be driven out of this saturated regime by increasing the gate voltage above a limiting value. For $V_{gs} - V_{th} \gtrsim V_{ds}/2$ the gate conductance is so high w.r.t. the conductance in the polyelectrolyte that a variation of this gate voltage will no longer result in a change of the source-drain current. This

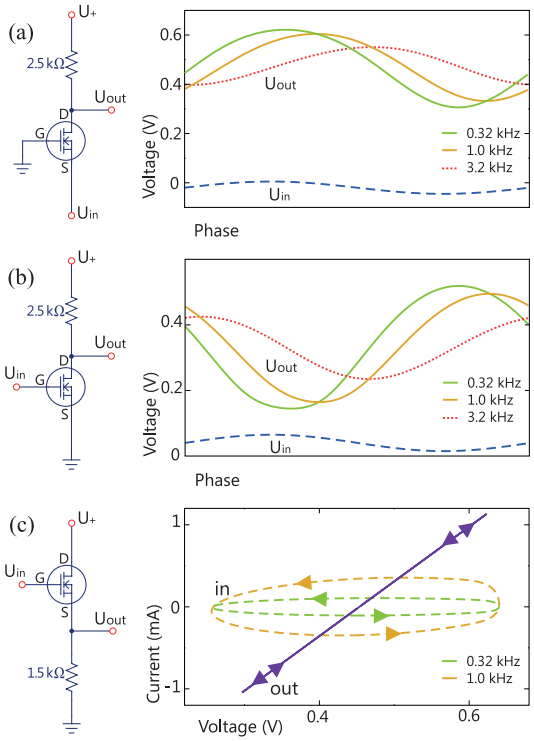

Fig. 4 The fundamental FET amplifier circuits, which are drawn schematically on the left, and the corresponding input (dashed line) and output signals for different frequencies (full and dotted lines) on the right, plotting the corresponding input/output voltages as a function of the phase of the sinusoidal input signal for the in (a) common-gate amplifier(a) and the common-source amplifier (b). For the case of the common-drain amplifier (c), we instead plot the gate voltage versus the gate current (in) as well as the source voltage versus the source current (out). Here, the output voltage and current are drawn shifted by $+0.07$ V and -0.25 mA for comparison of the signals.

defines a third, *ohmic mode* for which the FEiT can best be described as a resistor. Tantalizingly, the division of the parameter space spanned by $V_{\rm ds}$ and $V_{\rm gs}$ into three fundamentally different modes, as is illustrated in the inset of Figure 3, shows a stunning analogy to the operation of the electronic FET. There are however some differences; the current in the ohmic mode is dependent on $V_{\rm gs}$ for the electronic FET yet independent on $V_{\rm gs}$ for the ionic transistor. Furthermore, in the active mode $j_{\rm ds}$ varies approximately linear with $V_{\rm gs}-V_{\rm th}$ for the ionic transistor whilst quadratically for the electronic FET. The latter implies that for the FEiT in the active mode the *transconductance* $g=\partial I_{\rm ds}/\partial V_{\rm gs}$, where $I_{\rm ds}=j_{\rm ds}eA$ is the electronic drain-source current, is approximately fixed to $g\approx j^*_{\rm ds}e^2A/kT$.

The observation that the FEiT can be put in the active mode for which a transconductance that is independent on $V_{\rm ds}$ is properly definable, naturally poses the question of whether or not the FEiT could be used in amplifiers, analogous to semiconductor transistors. To that end, we consider the three most fundamental amplifier circuits that can be constructed with field-effect transistors. The working of these crucially rely on FETs that operate in the active mode. Here, we consider an FEiT at the heart of each of the circuits and numerically simulate these by solving the Nernst-Planck equations dynamically w.r.t. the parameters $V_{\rm ds}$ and $V_{\rm gs}$ and coupling the resulting currents back into the circuit. Biasing the transistor into the active mode can be accomplished by the choice of the resistors and the offset voltages for the sine-wave input voltage $U_{\rm in}$. We will use $A=1$ mm^2, which yields $j^*_{\rm ds}eA=1.6$ mA. Diagrams corresponding to each amplifier circuit showing the FEiT with all its electrodes (D,G,S) as well as a resistor are shown on the left side in Figure 4. In (a) we show the circuit diagrams and the results for the common-gate amplifier configuration which was realised by grounding the gate electrode, connecting the drain to a $U_+=0.76$ V positive voltage source through a $2.5k\Omega$ resistor, and applying an oscillating input voltage $U_{\rm in}$ at the source. The right figure shows as a function of the phase the input signal $U_{\rm in}$ as a dashed line and the resulting output signals $U_{\rm out}$ for three different signal frequencies as full lines. Auspiciously, we observe an amplification of approximately 6 times here, up to frequencies of about 10^2-10^3 Hz, above which the phase and amplitude shift of the output signal becomes too significant. Generally speaking, the common-gate amplifier circuit however finds little use since it draws undesirably large currents from the input. A much more customary amplifier configuration is therefore the common-source amplifier. Here, the source is grounded and an input signal is applied to the gate. The result is an inverted and amplified signal at the drain. Our numerical simulations confirm that this amplifier can be realized with the FEiT as well. As Figure 4b shows, the observed (inverted) amplification factor for this circuit is similar to that of the common-gate circuit. The third amplifier circuit that can be constructed with field-effect transistors is the common-drain amplifier and this circuit finds use as a voltage follower which mirrors input signals to a loaded output while keeping the currents from (or to) the input minimal. In Figure 4c we show that the drain is being connected to the positive voltage source, the source is grounded via a load $R=1.5k\Omega$ and the input signal is applied to the gate. Our numerical data corresponding to this circuit confirm that the output signal follows the input approximately one-to-one. By design, the output current is linear in the voltage and consequently yields a straight line in the voltage-current plot, yet for moderate frequencies only a relatively small current is drawn to or from the input. This is demonstrated by the almost entirely horizontal cycles in Figure 4c, which plots the input current

and the output current as a function of the alternating voltage at the corresponding electrodes. The latter confirms that also in the third of these three amplifier configurations the FEiT can be applied. Our results therefore indicate the existence of a well-defined frequency regime in which the FEiT can be used to construct each amplifier of choice. The observed breakdown frequency is in agreement with the assumption that the characteristic inverse time scale D_g/L_g^2 limits the operating frequency of the device. This relation, which we have confirmed by calculations using other FEiT system parameters, shows that a decrease of the system size towards the nanometre scale is expected to result in an increase of the maximum frequency by a few orders of magnitude. Our numerical calculations also demonstrate that it will be advantageous in this respect to search for soft materials that are characterised by relatively fast ion diffusion, as a higher effective ion diffusion constant in the gate area will enable the transistor to operate at higher frequencies. Furthermore, as Equation (3) indicates, the effective ion diffusion constant in the polyelectrolyte will linearly relate to the threshold current density.

To summarize, by using Nernst-Planck numerical simulations as well as an analytical approach based on the variation in the chemical potential we demonstrated that ionic analogues of the electronic field-effect transistor can show sub-threshold, active and ohmic operational modes, which yields the possibility of constructing ionic signal-amplifying circuits from soft materials. The relation between the redox electrodes half-cell potentials, the gate material work function, and the polyelectrolyte charge density will be of crucial relevance for the characteristic FET properties such as the threshold voltage and the transconductance, which determine fundamentally the current response to applied voltage differences. By considering alternative redox reactions, complimentary devices could also be investigated, having the cation as the charge carrier. This could lead to energy-efficient ionic CMOS technology. Our model is exploratory and can guide future experiments.

1 Acknowledgements

This work was supported by the Center for Bio-Inspired Energy Science (CBES), which is an Energy Frontier Research Center funded by the U.S. Department of Energy, Office of Science, Office of Basic Energy Sciences under Award Number DE-SC0000989. We thank Andrew Koltonow for useful suggestions.

References

1 M. E. Roberts, S. C. B. Mannsfeld, N. Queralt, C. Reese, J. Locklin, W. Knoll, and Z. Bao, PNAS **105**, 12134 (2008).
2 B. P. Pal, B. M. Dhar, S. K. C., and H. E. Katz, Nat. Mater. **8**, 898 (2009).
3 A. C. Arias, J. D. MacKenzie, I. McCulloch, J. Rivnay, and A. Salleo, Chem. Rev. **110**, 3 (2010).
4 Y.-g. Ha, J. D. Emery, M. J. Bedzyk, H. Usta, A. Facchetti, and T. J. Marks, J. Am. Chem. Soc. **133**, 10239 (2011).
5 A. Facchetti, Chem. Mater. **23**, 733 (2011).
6 K. H. Lee, M. S. Kang, S. Zhang, Y. Gu, T. P. Lodge, and C. D. Frisbie, Advanced Materials **24**, 4457 (2012).
7 M. Irimia-Vladu, E. D. Glowacki, G. Voss, S. Bauer, and N. S. Sariciftci, Materials Today **15**, 340 (2012).
8 L. M. Dumitru, K. Manoli, M. Magliulo, T. Ligonzo, G. Palazzo, and L. Torsi, APL Materials **3**, 014904 (2015).
9 C. Keplinger, J.-Y. Sun, C. C. Foo, P. Rothemund, G. M. Whitesides, and Z. Suo, Science **341**, 984 (2013).
10 D. A. Bernards, S. Flores-Torres, A. na H. D., and G. G. Malliaras, Science **8**, 1416 (2006).
11 J.-H. Han, K. Kim, H. Kim, and T. Chung, Angew. Chem. Int. Ed. **48**, 3830 (2009).
12 J. Am. Chem. Soc. pp. 10801–10806 (2007).
13 H. Nakanishi, D. A. Walker, K. J. M. Bishop, P. J. Wesson, Y. Yan, S. Soh, S. Swaminathan, and B. A. Grzybowski, Nat. Nanotechnol. **6**, 740 (2011).
14 R. S. Eisenberg, Fluct. Noise Lett. **11**, 76 (2012).
15 R. Fan, H. Seong, R. Yan, J. Arnold, and P. Yang, Nat. Mater. **7**, 303 (2008).
16 S. M. Sze and K. K. Ng, *Physics of Seimiconductor Devices* (John Wiley & Sons, 2007).
17 P. Simon and Y. Gogotsi, Nat. Mater. (2008).
18 M. D. Levi, G. Salitra, N. Levy, D. Aurbach, and J. Maier, Nat. Mater. **8** (2009).
19 D. Brogioli, Phys. Rev. Lett. **103**, 058501 (2009).
20 N. Boon and R. van Roij, Mol. Phys. **109**, 1229 (2011).
21 Y. Oren, Desalination **228**, 10 (2008).
22 B. Mi, Science **343**, 740 (2014).
23 A. E. Javier, S. N. Patel, D. T. Hallinan, V. Srinivasan, and N. P. Balsara, Angew. Chem. Int. Ed. **50**, 9848 (2011).
24 C. E. Sing, J. W. Zwanikken, and M. Olvera de la Cruz, Nat. Mater. **13**, 694 (2014).
25 D. T. Hallinan and N. P. Balsara, Annu. Rev. Mater. Res. **43**, 503 (2013).
26 H. Reiss, J. Phys. Chem. **89**, 3783 (1985).
27 C. Kittel, *Introduction to Solid State Physics* (Wiley, New York, ????).
28 H. H. Girault, *Analytical and Physical Electrochemistry*

(EPFL Press, 2004).
29 H. Reiss and A. Heller, J. Phys. Chem. **89**, 4207 (1985).
30 R. G. Bates and J. B. Macaskill, Pure & Appl. Chem. **50**, 1701 (1978).
31 P. M. Biesheuvel and M. Z. Bazant, Phys. Rev. E **81**, 031502 (2010).
32 M. Mirzadeh, F. Gibou, and T. M. Squires, Phys. Rev. Lett. **113**, 097701 (2014).
33 S. Kondrat, P. Wu, R. Qiao, and A. A. Kornyshev, Nat. Mater. **13**, 387 (2014).
34 P. M. Biesheuvel, Y. Fu, and M. Z. Bazant, Phys. Rev. E **83**, 061507 (2011).
35 S. Suzuki, C. Bower, Y. Watanabe, and O. Zhou, Appl. Phys. Lett. **76**, 4007 (2000).
36 I. Ferain, C. A. Colinge, and J.-P. Colinge, Nature **479** (2011).